Original Research

PSD-95 protects the pancreas against pathological damage through p38 MAPK signaling pathway in acute pancreatitis

Yinan Guo[1], Weikai Hu[2], Xueyan Wang[2], Chunyun Li[2], Tianyu Cui[2], Ruixia Liu[1], Junqi He[3] and Chenghong Yin[2]

[1]Central Laboratory, Beijing Obstetrics and Gynecology Hospital, Capital Medical University, Beijing 100026, China; [2]Department of Internal Medicine, Beijing Obstetrics and Gynecology Hospital, Capital Medical University, Beijing 100026, China; [3]Department of Biochemistry and Molecular Biology, Capital Medical University, Beijing 100069, China

Corresponding author: Chenghong Yin. Email: yinchh@ccmu.edu.cn; Junqi He. Email: jq_he@ccmu.edu.cn; Ruixia Liu. Email: liuruixia@ccmu.edu.cn

Impact statement

AP is a common clinical acute abdominal disease, while the pathogenesis of the inflammatory response and pancreatic pathological damage of it has not been fully elucidated. PSD-95 is widely distributed in brain tissues and is one of the most important and abundant scaffolding proteins in the postsynaptic membrane. However, only a few studies have focuses on the function of PSD-95 in inflammatory disorders in other tissues and organs. In this study, we confirmed that PSD-95 was detectable in pancreatic acinar cells, and played an important role in decreasing the process of edematous AP *in vivo* and *in vitro* for the first time. We also showed that PSD-95 could statistically reduce the histopathological lesions of edematous AP through the p38 MAPK signaling pathway. We aim to continue exploring how PSD-95 regulates the inflammatory response of AP, along with the relationship between PSD-95 and p38 MAPK in AP. These findings uncover a new target for future studies that may result in new AP-related treatments in the future.

Abstract

Acute pancreatitis is one of the leading causes of gastrointestinal disorder-related hospitalizations, yet its pathogenesis remains to be fully elucidated. Postsynaptic density protein-95 (PSD-95) is closely associated with tissue inflammation and injury. We aimed to investigate the expression of PSD-95 in pancreatic acinar cells, and its function in regulating the inflammatory response and pancreatic pathological damage in acute pancreatitis. A mouse model of edematous acute pancreatitis was induced with caerulein and lipopolysaccharide in C57BL/6 mice. Tat-N-dimer was injected to inhibit the PSD-95 activity separately, or simultaneously with SB203580, inhibitor of p38 MAPK phosphorylation. Rat pancreatic acinar cells AR42J were cultured with 1 μM caerulein to build a cell model of acute pancreatitis. PSD-95-knockdown and negative control cell lines were constructed by lentiviral transfection of AR42J cells. Paraffin-embedded pancreatic tissue samples were processed for routine HE staining to evaluate the pathological changes of human and mouse pancreatic tissues. Serum amylase and inflammatory cytokine levels were detected with specific ELISA kits. Immunofluorescence, immunohistochemical, Western-blot, and qRT-PCR were used to detect the expression levels of PSD-95, p38, and phosphorylated p38. Our findings showed that PSD-95 is expressed in the pancreatic tissues of humans, C57BL/6 mice, and AR42J cells, primarily in the cytoplasm. PSD-95 expression increased at 2 h, reaching the peak at 6 h in mice and 12 h in AR42J cells. IL-6, IL-8, and TNF-α increased within 2 h of disease induction. The pancreatic histopathologic score was greater in the PSD-95 inhibition group compared with the control ($P < 0.05$), while it was lesser when phosphorylation of p38 MAPK was inhibited compared with the PSD-95 inhibition group ($P < 0.05$). Moreover, phosphorylation of p38 MAPK increased statistically after PSD-95 knocked-down. In conclusion, PSD-95 effectively influences the pathological damage of the pancreas in acute pancreatitis by affecting the phosphorylation of p38 MAPK.

Keywords: Acute pancreatitis, PSD-95, inflammation, p38 mitogen-activated protein kinases, pathological damage

***Experimental Biology and Medicine* 2021; 246: 1473–1482. DOI: 10.1177/15353702211003293**

Introduction

Acute pancreatitis (AP) is a common clinical acute abdominal disease and is one of the leading causes of gastrointestinal disorders-related hospitalizations.[1] The frequency of AP is increasing worldwide, while the mortality increases with age.[2] The inflammatory cascade is often activated by local damage of the pancreas, which may subsequently lead to systemic inflammatory response syndrome (SIRS) and multiorgan dysfunction syndrome (MODS). Both SIRS and MODS are the main causes of morbidity and mortality

in AP. The pathophysiology of AP incorporates both the local damage of the pancreas and the systemic inflammatory response.[3–5] However, the pathogenesis of the inflammatory response and pancreatic pathological damage of AP has not been fully elucidated.

Postsynaptic density protein-95 (PSD-95) is widely distributed in brain tissues and is one of the most important and abundant scaffolding proteins in the postsynaptic membrane, while very few studies have evaluated the expression of PSD-95 in other organs. The main function of PSD-95 is participating in the formation of synaptic connections, maintenance of synaptic plasticity, and the aggregation of multiple receptors.[6–8] Besides, PSD-95 is also closely associated with tissue inflammation and injury in some diseases. For example, a recent study found that PSD-95 is reduced in the hippocampus of a mouse model of neuroinflammation induced by LPS.[9] Moreover, NR2B antagonists can effectively inhibit the assembly of the NR2B-CaMKII-PSD95 signal module, and protect neuron injury against LPS-induced inflammation in mice.[10] This indicated that PSD-95 is relevant to brain injury induced by LPS. However, there are few studies on the function of PSD-95 in diseases outside of nervous system. As the inflammatory response is a critical process of AP, further studies are needed to elucidate the possible mechanism.

P38 mitogen-activated protein kinases (MAPK) are one of the serine/threonine-protein kinase family members. P38 MAPK regulates several cellular responses, including inflammation, cell cycle, differentiation, senescence, apoptosis, and tumorigenesis. The MAPK signaling pathway is a potential target of inflammation-related therapies.[11] Studies have shown that p38 MAPK is also involved in the regulation of AP.[12–14] In addition, PSD-95 has been shown to affect the phosphorylation of p38 MAPK in the neural tissue,[15,16] suggesting that p38 MAPK may be involved in a downstream pathway of PSD-95.

In the current study, we aimed to investigate the expression of PSD-95 in pancreatic tissues and acinar cells, including its role in protecting pancreatic tissue damage and regulating the inflammatory response in AP. Lastly, we aimed to assess the relationship of PSD-95 and p38 MAPK to determine whether PSD-95 plays its role through the p38 MAPK pathway in AP.

Materials and methods

AP mouse model

Animal experiments were approved by the Animal Welfare and Ethics Committee of Capital Medical University (AEEI-2018–074) and performed according to the Declaration of Helsinki. C57BL/6 mice (male, eight weeks, 25 ± 5 g) were purchased from Beijing Vital River Laboratory Animal Technology Co., Ltd (Beijing, China). Edematous AP was induced in mice, as previously described.[17] Briefly, mice were randomly assigned to different groups ($n = 5$ per group), and received intraperitoneal injections (100 μg/kg) of CAE (Sigma, St. Louis, MO, USA) at 1-h intervals for 6 h. Next, the mice were injected intraperitoneally with LPS at 50 μg/kg (Sigma, St. Louis, MO, USA) immediately after the final CAE injection. The PSD-95 inhibitor, Tat-N-dimer, was injected after LPS injection at 3 nmol/g in the PSD-95 inhibition groups, as previously reported.[18] SB203580 was injected with Tat-N-dimer simultaneously to inhibit p38 MAPK phosphorylation. The mice were sacrificed at 0.5 h, 2 h, 6 h, 12 h, 24 h, and 48 h after the final intraperitoneal injection. Mice of the PSD-95 and p38 MAPK inhibition groups were killed at 2 h and 6 h post-injection, because PSD-95 increased at 2 h and reached its peak at 6 h post-injection. Intraperitoneal injection of pentobarbital sodium was used for anesthesia (0.1 mg/g, Merck & Co., Inc., Darmstadt, Germany).

Histological evaluation

The tissues adjacent to pancreatic cancer of human were acquired from the Biological Samples and Clinical Information Repository of Beijing Friendship Hospital, Capital Medical University. All procedures were performed in accordance with the Ethical Guidelines for Human Genome/Gene Research enacted by the Chinese Government, which was approved by the Ethics Committee of Capital Medical University (Approval ID: BJFH-EC/2014–040). Pancreatic tissues, and other organ tissues of mice were harvested and placed into liquefied nitrogen or 10% buffered formalin for subsequent analysis. For histological evaluation, pancreatic tissues were embedded in paraffin and sliced into 4 μM sections. Hematoxylin and eosin (HE) staining was used to evaluate the pathological changes in the tissues.[17] The histopathologic grade was evaluated, with reference to the standard from Schmidt *et al.*[19] in 1992.

Determination of serum amylase and inflammatory cytokine levels

Blood samples were collected from the medial canthus vein of each mouse and stored at −80°C for analysis by enzyme-linked immunosorbent assay (ELISA) kits. The expression level and activity of serum amylase, as well as serum levels of tumor necrosis factor-α (TNF-α), interleukin-6 (IL-6), IL-8, and IL-10 were determined with specific ELISA kits (Abcam, Cambridge, England, UK and Research and Diagnosis Systems, Minneapolis, MN, USA) according to the manufacturer's instructions.

Cell culture

Rat pancreatic acinar cells AR42J (ATCC, Rockville, MD, USA) were cultured in F12K medium containing 20% fetal bovine serum, 100 U/mL penicillin, and 100 mg/mL streptomycin under standard conditions, with 5% CO_2 at 37°C. All experiments were carried out at least 24 h after the cells were seeded. The cells were stimulated with 1 μM CAE (Sigma, St. Louis, MO, USA) for 2 h, 6 h, 12 h, 24 h, or 48 h to build the AP cell model, as previously described.[20]

Lentivirus transfection of cells

PSD-95 knockdown (AR42J-PSD-95-KD) and its negative control cells (AR42J-NC) were both generated with the

AR42J cell line. First, the cells were seeded in the 96-well culture plates at 4000 cells per well. The PSD-95-RNAi sequence (GACCGACGACATTGGCTTCAT) was designed based on the full-length rat PSD-95 cDNA sequence and cloned into the GV298 vector with cherry fluorescence and puromycin-resistant cassette (GeneChem Co. Ltd, Shanghai, China). A non-silencing-siRNA (NS-siRNA, TTCTCCGAACGTGTCACGT) was used as the negative control. At 24 h post-transfection, the cherry fluorescent protein was detectable by fluorescent microscopy, and stable AR42J-PSD-95-KD cells were selected with 2.5 μM puromycin (Sigma-Aldrich, St. Louis, MO, USA). Puromycin-resistant clones were obtained after several weeks. PSD-95 expression was examined by Western blot analysis.

Immunofluorescence

Immunofluorescence was used to detect the presence of PSD-95 in AR42J cells. AR42J cells were rinsed in phosphate-buffered solution (PBS) and fixed in 4% (v/v) paraformaldehyde (40 min, 37°C) after the cells were seeded on the slides in 24-wells culture plates for 24 h. Next, the cells were then incubated with primary antibody (ab2723 [1:200], Abcam, Cambridge, England, UK) overnight at 4°C. After rinsing with PBS, cells were incubated with the secondary antibody (FITC [1:500] green fluorescent) (Sigma, St Louis, MO) for 1 h at room temperature. The fluorescent dye, 4′,6-diamidino-2-phenylindole (DAPI), was used to stain the cell nuclei (blue). Some sections were incubated with normal goat serum instead of the primary antibody to create the negative controls.

Quantitative real-time polymerase chain reaction analysis

Total RNA was extracted from AR42J cells and pancreatic tissues of mice in each group using the TRIzol reagent (Invitrogen, Carlsbad, CA, USA). The first-stranded cDNA was obtained from total RNA with the Transcriptor cDNA Synthesis kit (Roche, Switzerland). The resultant cDNA was subjected to qRT-PCR with specific primers as follows: mouse PSD-95 (Forward, 5′- ATGTGCTTCATG TAATTGACGC-3′, and reverse, 3′-TTTAACCTTGACCAC TCTCGTC-5′), rat PSD-95 (Forward, 5′-TCCAGTCTGTG CGAGAGGTAGC-3′, and reverse, 3′-GGACGGATGAAG ATGGC-GATGG-5′). The PCR analysis was performed with a Power SYBR Green PCR Master Mix (Applied Biosystems, Foster City, CA, USA) in an Applied Biosystems 7500 platform. The PCR conditions were as follows: denaturation at 95°C for 5 min, 40 cycles of 95°C for 15 s, and 60°C for 1 min. GAPDH cDNA was used to normalize the sample amounts for the quantitative analysis.

Immunohistochemistry

The localization of PSD-95 in the pancreas was detected with immunohistochemical (IHC) staining. The heat-induced antigens were unmasked by microwaving the slides in citrate buffer (pH 6.0) for 10 min at 98°C. To suppress endogenous peroxidase and pseudo-peroxidase activity, the sections were treated with 3% hydrogen peroxide in methanol for 10 min at room temperature. After rinsing the slides in PBS, the sections were incubated with PSD-95 (1:200 dilution) antibodies overnight at 4°C. Normal rabbit serum (1:10 dilution) was used as the negative control. Next, the sections were incubated with polyperoxidase-conjugated secondary antibody for 30 min at room temperature, after rinsing the sections in PBS. Color development was accomplished with diaminobenzidine tetrachloride (DAB), while HE staining was performed to assess the tissues under light microscopy.

Western blot analysis

AR42J cells were collected in lysis buffer (Bioss, Beijing, China) on ice for 30 min after washing three times with cold PBS. Pancreatic tissues (30 mg) were chopped into fine fragments and placed into a centrifuge tube with 300 μL radio immunoprecipitation assay (RIPA) lysis buffer (Solarbio, Beijing, China) supplemented with proteinase inhibitors (Solarbio, Beijing, China). The tissue or cell lysates were centrifuged at 11,440*g* at 4°C for 10 min. Protein concentration was measured using the bicinchoninic acid (BCA) protein assay kit (Pierce Chemical Co., Rockford, IL, USA). Protein samples were separated by SDS-PAGE and transferred onto polyvinylidene fluoride (PVDF) membranes (Millipore, Darmstadt, Germany), which were incubated with 5% skim milk at 37°C for 1 h. The membranes were then probed with the target antibody in 5% (w/v) milk in tris-buffered saline with tween (TBS-T) overnight. Horseradish peroxidase-conjugated secondary antibodies were diluted at 1:4000. Signals were detected by the Image Lab software (170–8195) from BioRad (Hercules, CA, USA). For the detection of target proteins, mouse anti-PSD-95 antibody (ab2723, Abcam, Cambridge, England, UK) rabbit anti-p38 (9212S, CST, Danvers, CO, USA), and rabbit anti-pp38 (4511S, CST, Danvers, CO, USA) were used at the dilution of 1:1000. Each experiment of Western blot was performed at least three times.

Statistics

Results were presented as mean ± SD. Results were analyzed with SPSS 20.0 (IBM, Chicago, IL, USA), and the Student's *t*-test or one-way ANOVA test was used to analyze the differences between groups. $P < 0.05$ was considered to be statistically significant.

Results

PSD-95 is highly expressed in the pancreas of mice

As shown in Figure 1, Western blot analysis revealed that PSD-95 is highly expressed in the stomach, colon, pancreas, and brain tissues of mice. However, PSD-95 expression is low in the lung, liver, and kidney tissues. PSD-95 expression is undetectable in skeletal muscle tissues.

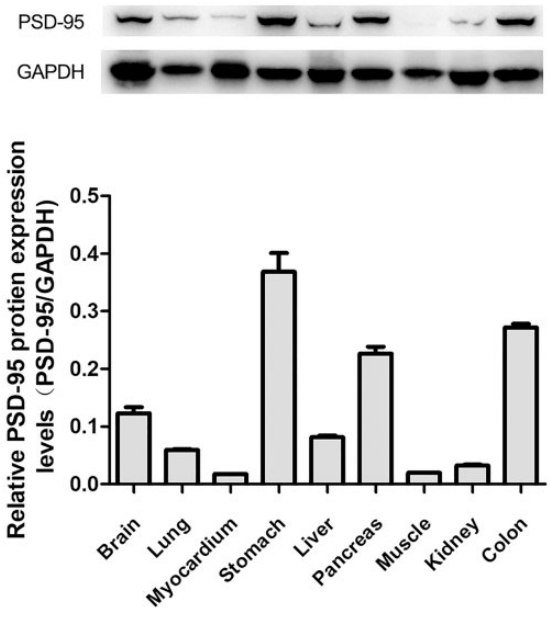

Figure 1. PSD-95 expression levels in different organs of C57BL/6 mouse. As shown through quantitative Western blot analysis, PSD-95 is highly expressed in the stomach, colon, pancreas, and brain tissues. PSD-95 is expressed at low levels in lung, liver, and kidney tissues. PSD-95 was undetectable in skeleton muscle tissues.

Histopathologic scores of pancreatic tissues, along with serum amylase and inflammatory factor levels in the pancreatic tissues from the edematous AP mouse model

Histopathologic indicators of edema, hemorrhage, and necrosis are observed in the pancreatic tissues from the AP group (Figure 2(a) to (d)). The histopathologic score was significantly higher at 2 h after disease induction, as compared with the control group ($P < 0.05$). However, the score gradually reduced from 2 to 48 h after disease induction (Figure 2(e)). Serum amylase expression levels were significantly increased in the AP group, as compared with the control group at 2 and 6 h after disease induction. The levels peaked at 12 h after disease induction ($P < 0.05$) (Figure 2(f)). Serum amylase activity was also significantly increased in the AP group, as compared with the control group at 2, 6, 12, and 24 h after disease induction. The levels peaked at 12 h after disease induction ($P < 0.05$) (Figure 2 (g)). IL-6, IL-8, and TNF-α increased by 2 h after disease induction, and then decreased gradually (Figure 2(h) to (j)). While IL-10 was significantly higher at 2 h after disease induction, the value decreased to its lowest level at 6 h after disease induction, followed by a gradual increase (Figure 2(k)).

Pancreatic PSD-95 expression is correlated with edematous AP in vitro and in vivo

PSD-95-specific staining is primarily localized in the cytoplasm of acinar cells in the pancreatic tissues of mice (Figure 3(d)) and humans (Figure 3(e)). Pancreatic PSD-95 protein levels were significantly higher in the AP group than the control group between 2 and 12 h after disease induction, peaking at 6 h ($P < 0.05$) (Figure 3(h)). Changes in mRNA levels of PSD-95 were associated with the concentration of the PSD-95 protein (Figure 3(i)). To confirm the results *in vitro*, immunofluorescence assays showed that PSD-95 is detectable in the cytoplasm of AR42J cells (Figure 3(a) to (c)). The PSD-95 protein level is higher in the AP group than the control group between 6 and 48 h ($P < 0.05$). In addition, PSD-95 protein levels peaked at 6 h after disease induction, and then gradually decreased (Figure 3(f)). Concurrently, there was a significant increase in PSD-95 mRNA levels between 2 and 6 h ($P < 0.05$) (Figure 4(g)), suggesting that PSD-95 may be correlated with the progression of edematous AP.

PSD-95 effectively reduces the pathological damage of the pancreas in edematous AP

HE staining of pancreatic tissues from the AP mice and PSD-95 inhibition group is shown in Figure 4(a) to (e). Histopathologic indicators of edema, hemorrhage, and necrosis are observed in pancreatic tissues of mice after inhibition of PSD-95, which is higher than the AP group at 2 h after disease induction. The histopathologic score was also significantly increased at 2 h in comparison with the control group ($P < 0.05$) (Figure 5(f)). Serum amylase expression levels and activity were both significantly increased after PSD-95 inhibition at 2 h (Figure 4(g) to (h)). While serum IL-6 was decreased after PSD-95 inhibition at both 2 and 6 h post-disease induction, there were no significant changes in IL-8 or TNF-α (Figure 4(i) to (k)). Hence, these findings demonstrate the significant effects of PSD-95 on the pathological damage of the pancreas in edematous AP.

P38 MAPK phosphorylation is negatively affected by PSD-95 in pancreatic acinar cells

PSD-95 is successfully knocked-down in AR42J cells (Figure 5(a) and (b)). In addition, p38 MAPK and phospho-p38 MAPK were detected in AR42J, AR42J-PSD-KD, and AR42J-NC cell lines. Pp38 expression increased significantly in the PSD-95-knockdown-AR42J cells, while there was no difference in total p38 between the PSD-95-knockout-AR42J cells and control cells (Figure 5(c) and (d)). Hence, the role of PSD-95 in AP may be mediated by p38 MAPK.

P38MAPK is required for PSD-95 to protect the pancreas from pathological damage

HE staining of pancreatic tissues from the AP group and inhibition group is shown in Figure 6(a). Results shown in Figure 6(b) demonstrate that the histopathologic score of Tat-N-dimer (+) and SB203580 (+) groups is significantly decreased compared with Tat-N-dimer (+) and SB203580 (−) groups ($P < 0.05$). The serum amylase expression levels and activity also reduced in the Tat-N-dimer (+) and SB203580 (+) groups ($P < 0.05$), as shown in Figure 6(c) and (d). Hence, SB203580 can reduce the Tat-N-dimer-mediated pathological damage and the of release serum amylase in edematous AP. In addition, these

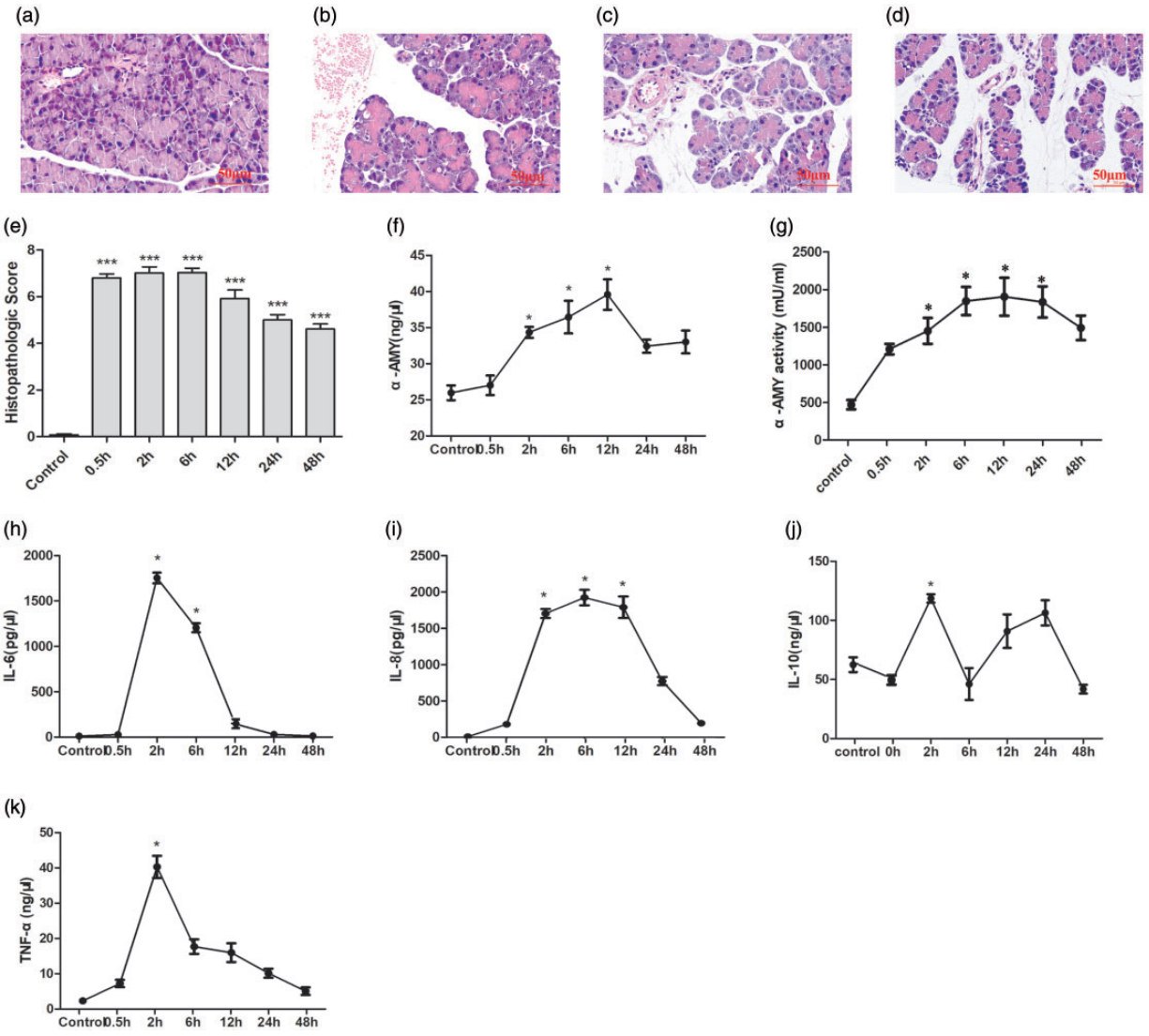

Figure 2. Assessment of hematoxylin and eosin (HE) staining, pathologic scores, and serum amylase and inflammatory factor levels in the pancreatic tissues from the acute pancreatitis (AP) mouse model (The scale bars, 50 μM). (a) Control group; (b) AP 0.5 h; (c) AP 2 h; (d) AP 6 h; (e) Relative pathologic score was significantly higher by 2 h after disease induction, as compared with the control group ($P < 0.05$), which gradually decreased by 48 h after disease induction. (f) Serum amylase expression levels. (g) Serum amylase activity. (h) Interleukin-6 (IL-6). (i) Interleukin-8 (IL-8). (j) Tumor necrosis factor-α (TNF)-α. (k) Interleukin-10 (IL-10) ($n = 5$ per group, $^*P < 0.05$ vs. control group). (A color version of this figure is available in the online journal.)

findings suggest that p38 MAPK is involved in how PSD-95 regulates the pathological damage of edematous AP.

Discussion

In this study, we explored the function of PSD-95 in edematous AP using both *in vitro* and *in vivo* models. We confirmed that PSD-95 is expressed in normal pancreatic and AP tissues. In addition, we showed that the pancreatic acinar cell AR42J also expressed PSD-95. Next, we investigated whether PSD-95 could reduce the histopathological pancreatic lesions in the mouse model of edematous AP. Furthermore, PSD-95 expression was closely associated with serum amylase and IL-6 levels in the edematous AP mouse model. Finally, we demonstrated that the phosphorylation of p38 MAPK was involved in how PSD-95 protects the pancreas from pathological damage.

Our study firstly indicated that PSD-95 was detectable in the pancreas of both human and mice pancreatic tissues, and rat pancreatic acinar cells (AR42J). In mice tissues, PSD-95 is highly expressed in the stomach and colon pancreas, and brain tissues, along with low expression in the lungs, liver, and kidneys. However, PSD-95 was not detected in the skeletal muscle tissues. Previous studies have shown that PSD-95 is mainly present in glutamatergic synapses, as it participates in several diseases of the nervous system.[8,21] In this study, PSD-95 expression at the gene and protein levels both increased after 2 or 6 h post-disease induction until they peaked. Hence, PSD-95 likely plays an important role in decreasing the progression of edematous AP.

In this study, we confirmed that PSD-95 could significantly protect pancreatic tissues from damage, further indicating that PSD-95 may play an important role in the pathological progress of edematous AP. Moreover, PSD-95 could significantly reduce serum amylase expression levels

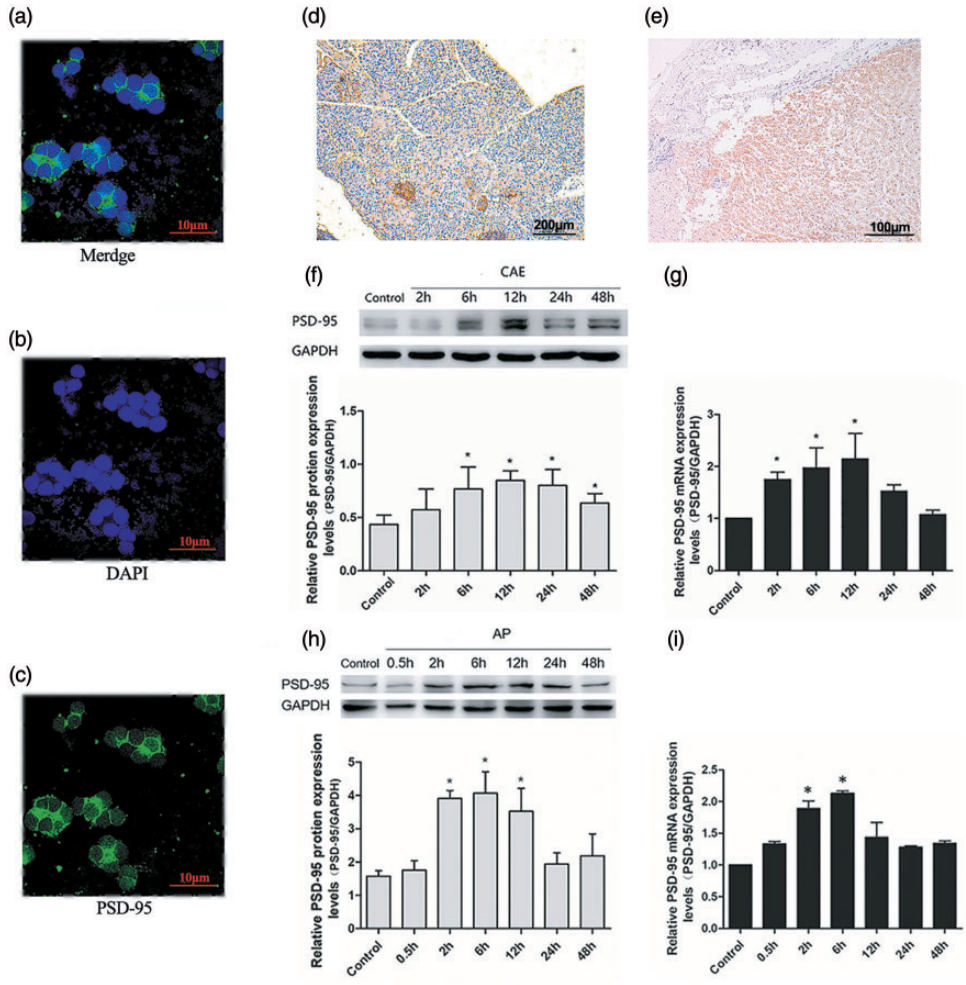

Figure 3. PSD-95 expression in AP mice and cell models. (a–c) PSD-95 localization in AR42J cell by immunofluorescence (the scale bars, 10 μM). (d) Immunohistology of PSD-95 in mouse pancreatic tissues (the scale bars, 100 μM); (e) Immunohistology of PSD-95 in tissues adjacent to cancer from pancreatic cancer patient (the scale bars, 200 μM). (f) Relative expression level of the PSD-95 protein in AR42J cells. (g) Relative expression level of PSD-95 mRNA in AR42J cells. (h) Relative expression level of PSD-95 protein in the AP mouse model. (i) Relative expression level of PSD-95 mRNA in the AP mouse model (*$P < 0.05$ vs. control group).

and activity in the edematous AP mouse model, and the expression of serum IL-6 was also influenced by PSD-95 expression. However, there were no changes in the expression of IL-8 or TNF-α. It was previously shown that early activation of trypsinogen might lead to localized tissue damage and the release of damage-associated molecular patterns (DAPMs).[22] This resulted in the recruitment of neutrophils and initiation of the inflammatory cascade was caused, which could ultimately lead to the increase of capillary permeability and damage of endothelium with microvascular thrombosis, causing MODS. Cytokines and chemokines were upregulated after the activation of pro-inflammatory transcription factor nuclear factor-κB (NF-κB), further amplifying the inflammatory response and the extent of pancreatic injury.[23,24] LPS-induced neuroinflammation studies have shown that PSD-95 is negatively related to the inflammatory response and closely associated with tissue injury.[9,10] The relationship between PSD-95 and inflammatory factors needs to be further explored.

Studies have indicated that p38 MAPK plays an important role in regulating inflammatory response,[25–27] as it was an upstream regulator of a variety of inflammatory cytokines, such as TNF-α, IL-1, and IL-6, which in return control the inflammatory response inside and outside cells.[28] There is a variety of signal transduction pathways involved in the development of AP inflammatory responses. The p38 MAPK signaling pathway was thought to regulate the inflammatory response in these signaling molecules.[29,30] In a previous study, Cao *et al.*[31] found that the p38 MAPK signaling pathway regulates the inflammatory response in AP. In another study, Zhu *et al.*[32] indicated that PAK1 inhibition alleviates CAE-induced AP by inhibiting p38 phosphorylation, also p65 transcription, phosphorylation, and translocation. Our previous studies showed that the Mas receptor effectively limited the inflammatory response of AP through the p38 MAPK/NF-κB signaling pathway.[20,33] Moreover, we have proved that SB203580, the inhibitor of p38 MAPK can down-regulate the expression levels of NF-κB, IL-6, TNF-α, and IL-8.[33]

In this study, we confirmed that PSD-95 could reduce the phosphorylation level of p38 MAPK in a cell model of AP. Similar results were reported in other studies. For example, Cao *et al.* [15] indicated that the PSD95-nNOS interaction

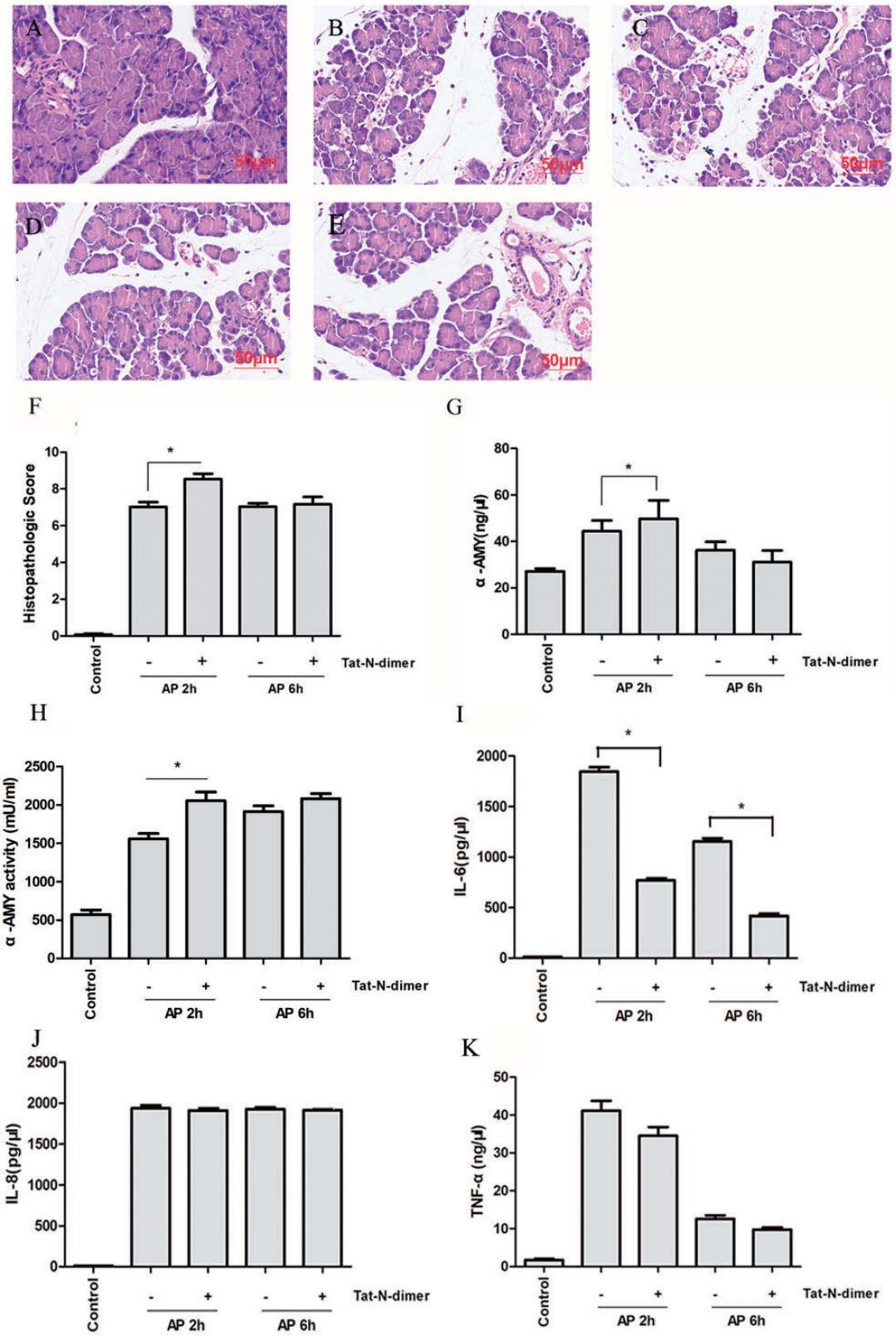

Figure 4. Effects of the PSD-95 inhibitor, Tat-N-dimer, in the AP mouse model. (a–g) HE staining and pathologic scores of the pancreatic tissues in AP mice after Tat-N-dimer induction(The scale bars, 50 μM); (a) Control; (b) AP 2 h; (c) AP 6 h; (d) PSD-95 inhibition 2 h; (e) PSD-95 inhibition 6 h; (f) Relative pathologic score of each group after Tat-N-dimer induction reveals that the histopathologic score is significantly higher at 2 h after PSD-95 was inhibited, as compared with the control group. (g–h) Serum amylase expression and activity were also increased significantly after PSD-95 was inhibited for 2 h; (i) Serum IL-6 expression level was decreased significantly after PSD-95 was inhibited for 2 and 6 h. (j–k) There were no significantly changes of the expression levels of serum IL-8 and TNF-α after PSD-95 was inhibited ($n = 5$ per group, $^*P < 0.05$ vs. control group). (A color version of this figure is available in the online journal.)

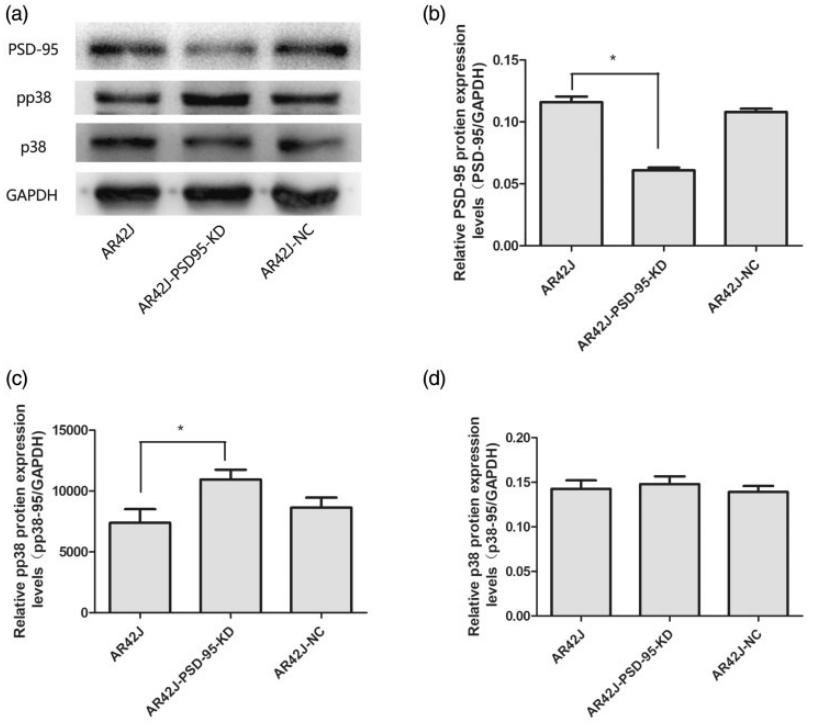

Figure 5. Effects of PSD-95 on p38 MAPK and phosphorylation of p38 MAPK. (a) PSD-95, p38 MAPK, and phospho-p38 MAPK (pp38) levels were detected in AR42J, AR42J-PSD-9D-KD, and negative control cells. (b) Relative expression levels of PSD-95 were significantly decreased in the AR42J-PSD-95-KD group. (c) Relative expression levels of pp38 were upregulated in the AR42J-PSD-95-KD group, as compared with the control group. (d) Total p38 MAPK expression was unchanged (*$P < 0.05$ vs. control group).

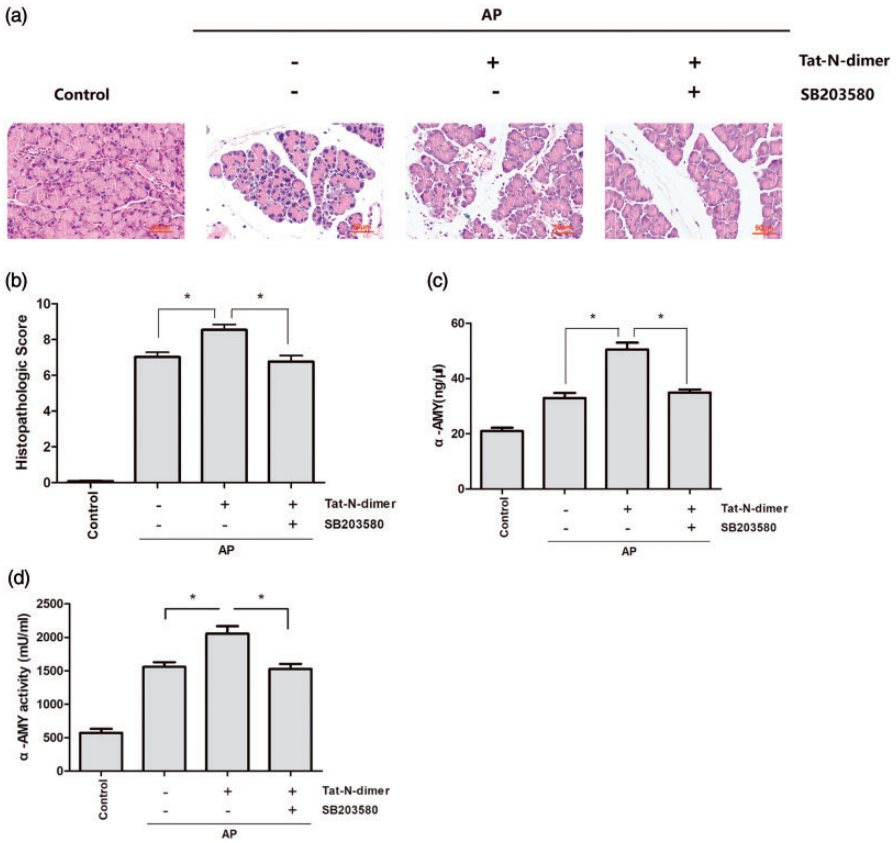

Figure 6. SB203580 inhibits Tat-N-dimer-mediated pathological damage and the rise of serum amylase expression and activity. (a) HE staining and pathologic scores of pancreatic tissues in AP mouse models after Tat-N-dimer and SB203580 induction for 2 h (the scale bars, 50 μM). (b) Relative pathologic scores demonstrate that SB203580 can effectively reduce the pathological damage caused by Tat-N-dimer in AP. (c–d) Serum amylase expression and activity levels verified our findings ($n = 5$ per group, *$P < 0.05$ vs. control group). (A color version of this figure is available in the online journal.)

subsequent NO production is critical for glutamate-induced p38 MAPK activation in cerebellar granule neurons. In another study, Qu *et al.* [16] showed that an inhibitor of nNOS-PSD95 (ZL006) could reduce the phospho-p38-positive neurons in the motor cortex. Hence, PSD-95 may regulate AP through the p38 MAPK signaling pathway. However, the findings of this study have to be seen in light of some limitations. The results of this study are based on the model of edematous AP. In consideration of the difference between edematous AP and necrotizing AP, this finding may not apply to the models of severe AP. Moreover, the exact mechanism is still unknown. A recent study demonstrated that PSD-95 could be combined with Mas, which would restrain the ubiquitin degradation of Mas.[34] Mas is a receptor for angiotensin (1–7) [Ang-(1–7)].[35] Studies showed that Ang-(1–7), by acting via Mas receptor, exerts inhibitory effects on inflammation and vascular and cellular growth mechanisms.[36,37] We recently found that Mas was detectable in pancreatic tissues of mice, and could effectively protect against pancreatic cell damage.[17,20] In addition, Mas could reduce the phospho-p38 levels in AP, as found in a previous study.[33] However, it is not clear if PSD-95 can affect phospho-p38 levels by reacting with Mas in AP. We plan to explore this topic in future studies.

Conclusions

In summary, we have confirmed that PSD-95 is associated with edematous AP *in vivo* and *in vitro*. We also showed that PSD-95 could significantly reduce the histopathological lesion of edematous AP through the p38 MAPK signaling pathway. We aim to continue exploring how PSD-95 regulates the inflammatory response of AP, along with the relationship between PSD-95 and p38 MAPK in AP, in the future. These findings uncover a new target for future studies that may result in new AP-related treatments in the future.

AUTHORS' CONTRIBUTIONS

All authors participated in the design, interpretation of the studies, and analysis of the data and review of the manuscript. GYN conducted experiments, and completed the manuscript. HWK and WXY conducted the molecular biology experiments. LCY and CTY were responsible for model building and data analysis. LRX, HJQ, and YCH supplied critical reagents, designed the study, and modified the manuscript.

DECLARATION OF CONFLICTING INTERESTS

The author(s) declared no potential conflicts of interest with respect to the research, authorship, and publication of this article.

FUNDING

The author(s) disclosed receipt of the following financial support for the research, authorship, and/or publication of this article: This study was supported by the Beijing Natural Science Foundation of [No.7182053]; the China Postdoctoral Science Foundation [No. 2018M631528]; and the Beijing Postdoctoral Research Foundation [2018-ZZ-104].

ORCID iD

Yinan Guo https://orcid.org/0000-0002-9595-7870

REFERENCES

1. Jenkins A, Shapiro J. Clinical guideline highlights for the hospitalist: initial management of acute pancreatitis in the hospitalized adult. *J Hosp Med* 2019;**14**:764–5
2. Colvin SD, Smith EN, Morgan DE, Porter KK. Acute pancreatitis: an update on the revised Atlanta classification. *Abdom Radiol* 2020;**45**:1222–31
3. de Pretis N, Amodio A, Frulloni L. Hypertriglyceridemic pancreatitis: epidemiology, pathophysiology and clinical management. *United Eur Gastroenterol J* 2018;**6**:649–55
4. Johnstone C. Pathophysiology and nursing management of acute pancreatitis. *Nurs Stand* 2018. doi: 10.7748/ns.2018.e11179. Epub ahead of print. PMID: 29952150.
5. Landahl P, Ansari D, Andersson R. Severe acute pancreatitis: gut barrier failure, systemic inflammatory response, acute lung injury, and the role of the mesenteric lymph. *Surg Infect* 2015;**16**:651–6
6. Cheng D, Hoogenraad CC, Rush J, Ramm E, Schlager MA, Duong DM, Xu P, Wijayawardana SR, Hanfelt J, Nakagawa T, Sheng M, Peng J. Relative and absolute quantification of postsynaptic density proteome isolated from rat forebrain and cerebellum. *Mol Cell Proteomics* 2006;**5**:1158–70
7. Chen L, Chetkovich DM, Petralia RS, Sweeney NT, Kawasaki Y, Wenthold RJ, Bredt DS, Nicoll RA. Stargazin regulates synaptic targeting of AMPA receptors by two distinct mechanisms. *Nature* 2000;**408**:936–43
8. Matt L, Kim K, Chowdhury D, Hell JW. Role of palmitoylation of postsynaptic proteins in promoting synaptic plasticity. *Front Mol Neurosci* 2019;**12**:8
9. Liu Y, Zhang Y, Zheng X, Fang T, Yang X, Luo X, Guo A, Newell KA, Huang XF, Yu Y. Galantamine improves cognition, hippocampal inflammation, and synaptic plasticity impairments induced by lipopolysaccharide in mice. *J Neuroinflammation* 2018;**15**:112
10. Song Y, Zhao X, Wang D, Zheng Y, Dai C, Guo M, Qin L, Wen X, Zhou X, Liu Z. Inhibition of LPS-induced brain injury by NR2B antagonists through reducing assembly of NR2B-CaMKII-PSD95 signal module. *Immunopharmacol Immunotoxicol* 2019;**41**:86–94
11. Kaminska B. MAPK signalling pathways as molecular targets for anti-inflammatory therapy – from molecular mechanisms to therapeutic benefits. *Biochim Biophys Acta* 2005;**1754**:253–62
12. Denham W, Yang J, Wang H, Botchkina G, Tracey KJ, Norman J. Inhibition of p38 mitogen activate kinase attenuates the severity of pancreatitis-induced adult respiratory distress syndrome. *Crit Care Med* 2000;**28**:2567–72
13. Kim DU, Bae GS, Kim MJ, Choi JW, Kim DG, Song HJ, Park SJ. Icariin attenuates the severity of cerulein induced acute pancreatitis by inhibiting p38 activation in mice. *Int J Mol Med* 2019;**44**:1563–73
14. Kim MJ, Kim DU, Choi JW, Kim DG, Song HJ, Bae GS, Park SJ. Silymarin attenuates the severity of cerulein-induced acute pancreatitis. *Pancreas* 2020;**49**:89–95
15. Cao J, Viholainen JI, Dart C, Warwick HK, Leyland ML, Courtney MJ. The PSD95-nNOS interface: a target for inhibition of excitotoxic p38 stress-activated protein kinase activation and cell death. *J Cell Biol* 2005;**168**:117–26
16. Qu W, Liu NK, Wu X, Wang Y, Xia Y, Sun Y, Lai Y, Li R, Shekhar A, Xu XM. Disrupting nNOS-PSD95 interaction improves neurological and cognitive recoveries after traumatic brain injury. *Cereb Cortex* 2020;**30**:3859–71
17. Wang Y, Wang J, Liu R, Qi H, Wen Y, Sun F, Yin C. Severe acute pancreatitis is associated with upregulation of the ACE2-angiotensin-(1-7)-

mas axis and promotes increased circulating angiotensin-(1-7). *Pancreatology* 2012;**12**:451–7
18. Kucharz K, Sondergaard RI, Bach A, Stromgaard K, Lauritzen M. PSD-95 uncoupling from NMDA receptors by Tat- N-dimer ameliorates neuronal depolarization in cortical spreading depression. *J Cereb Blood Flow Metab* 2017;**37**:1820–8
19. Schmidt J, Lewandrowski K, Fernandez-del CC, Mandavilli U, Compton CC, Warshaw AL, Rattner DW. Histopathologic correlates of serum amylase activity in acute experimental pancreatitis. *Dig Dis Sci* 1992;**37**:1426–33
20. Wang J, Liu R, Qi H, Wang Y, Cui L, Wen Y, Li H, Yin C. The ACE2-angiotensin-(1-7)-mas axis protects against pancreatic cell damage in cell culture. *Pancreas* 2015;**44**:266–72
21. Zeng M, Ye F, Xu J, Zhang M. PDZ ligand binding-induced conformational coupling of the PDZ-SH3-GK tandems in PSD-95 family MAGUKs. *J Mol Biol* 2018;**430**:69–86
22. Watanabe T, Kudo M, Strober W. Immunopathogenesis of pancreatitis. *Mucosal Immunol* 2017;**10**:283–98
23. Awla D, Abdulla A, Syk I, Jeppsson B, Regner S, Thorlacius H. Neutrophil-derived matrix metalloproteinase-9 is a potent activator of trypsinogen in acinar cells in acute pancreatitis. *J Leukoc Biol* 2012;**91**:711–9
24. Navarro S. Historical review of our knowledge of acute pancreatitis. *Gastroenterol Hepatol* 2018;**41**:143.e1–43.e10
25. Brown DS, Cumming JG, Bethel P, Finlayson J, Gerhardt S, Nash I, Pauptit RA, Pike KG, Reid A, Snelson W, Swallow S, Thompson C. The discovery of N-cyclopropyl-4-methyl-3-[6-(4-methylpiperazin-1-yl)-4-oxoquinazolin-3(4H)-yl]ben zamide (AZD6703), a clinical p38alpha MAP kinase inhibitor for the treatment of inflammatory diseases. *Bioorg Med Chem Lett* 2012;**22**:3879–83
26. Yong HY, Koh MS, Moon A. The p38 MAPK inhibitors for the treatment of inflammatory diseases and cancer. *Expert Opin Investig Drugs* 2009;**18**:1893–905
27. Gupta J, Nebreda AR. Roles of p38alpha mitogen-activated protein kinase in mouse models of inflammatory diseases and cancer. *FEBS J* 2015;**282**:1841–57
28. Zer C, Sachs G, Shin JM. Identification of genomic targets downstream of p38 mitogen-activated protein kinase pathway mediating tumor necrosis factor-alpha signaling. *Physiol Genom* 2007;**31**:343–51
29. Kyriakis JM, Avruch J. Mammalian MAPK signal transduction pathways activated by stress and inflammation: a 10-year update. *Physiol Rev* 2012;**92**:689–737
30. Chen Y, Zhao Q, Chen Q, Zhang Y, Shao B, Jin Y, Wu J. Melatonin attenuated inflammatory reaction by inhibiting the activation of p38 and NFkappaB in taurocholateinduced acute pancreatitis. *Mol Med Rep* 2018;**17**:5934–9
31. Cao MH, Xu J, Cai HD, Lv ZW, Feng YJ, Li K, Chen CQ, Li YY. p38 MAPK inhibition alleviates experimental acute pancreatitis in mice. *Hepatobiliary Pancreat Dis Int* 2015;**14**:101–6
32. Zhu M, Xu Y, Zhang W, Gu T, Wang D. Inhibition of PAK1 alleviates cerulein-induced acute pancreatitis via p38 and NF-kappaB pathways. *Biosci Rep* 2019;**39**:BSR20182221
33. Yu X, Cui L, Hou F, Liu X, Wang Y, Wen Y, Li CC, Liu C, Yin R. C. Angiotensin-converting enzyme 2-angiotensin (1-7)-mas axis prevents pancreatic acinar cell inflammatory response via inhibition of the p38 mitogen-activated protein kinase/nuclear factor-kappaB pathway. *Int J Mol Med* 2018;**41**:409–20
34. Bian W, Sun L, Yang L, Li JF, Hu J, Zheng S, Guo R, Feng D, Ma Q, Shi X, Xiong Y, Yang X, Song R, Xu J, Wang S, He J. Stabilization of the angiotensin-(1-7) receptor mas through interaction with PSD95. *Biochem J* 2013;**453**:345–56
35. Santos RA, Simoes e Silva AC, Maric C, Silva DM, Machado RP, de Buhr I, Heringer-Walther S, Pinheiro SV, Lopes MT, Bader M, Mendes EP, Lemos VS, Campagnole-Santos MJ, Schultheiss HP, Speth R, Walther T. Angiotensin-(1-7) is an endogenous ligand for the G protein-coupled receptor mas. *Proc Natl Acad Sci U S A* 2003;**100**:8258–63
36. Santos RA, Ferreira AJ, Simoes ESAC. Recent advances in the angiotensin-converting enzyme 2-angiotensin(1-7)-mas axis. *Exp Physiol* 2008;**93**:519–27
37. Simoes e Silva AC, Silveira KD, Ferreira AJ, Teixeira MM. ACE2, angiotensin-(1-7) and mas receptor axis in inflammation and fibrosis. *Br J Pharmacol* 2013;**169**:477–92

(Received September 13, 2020, Accepted February 26, 2021)